Synthesis, structure and dioxygen reactivity of a bis(μ-iodo)dicopper(I) complex supported by the [*N*-(3,5-di-*tert*-butyl-2-hydroxybenzyl)-*N*,*N*-di-(2-pyridylmethyl)]amine ligand†

Svetlana V. Pavlova,[a] Hing Lun To,[b] Edith S. H. Chan,[b] Hung-Wing Li,[b] Thomas C. W. Mak,[b] Hung Kay Lee*[b] and Sunney I. Chan*[a]

Received 30th September 2005, Accepted 25th January 2006
First published as an Advance Article on the web 14th February 2006
DOI: 10.1039/b513898a

The air-sensitive bis(μ-iodo)dicopper(I) complex **1** supported by [*N*-(3,5-di-*tert*-butyl-2-hydroxybenzyl)-*N*,*N*-di-(2-pyridylmethyl)]amine (L) has been prepared by treating copper(I) iodide with L in anhydrous THF. Compound **1** crystallizes as a dimer in space group *C*2/*c*. Each copper(I) center has distorted tetrahedral N_2I_2 coordination geometry with Cu–N(pyridyl) distances 2.061(3) and 2.063(3) Å, Cu–I distances 2.6162(5) and 2.7817(5) and a Cu···Cu distance of 2.9086(8) Å. Complex **1** is rapidly oxidized by dioxygen in CH_2Cl_2 with a 1 : 1 stoichiometry giving the bis(μ-iodo)peroxodicopper(II) complex $[Cu(L)(\mu\text{-}I)]_2O_2$ (**2**). The reaction of **1** with dioxygen has been characterized by UV-vis, mass spectrometry, EPR and Cu *K*-edge X-ray absorption spectroscopy at low temperature (193 K) and above. The mass spectrometry and low temperature EPR measurements suggested an equilibrium between the bis(μ-iodo)peroxodicopper(II) complex **2** and its dimer, namely, the tetranuclear (peroxodicopper(II))$_2$ complex $[Cu(L)(\mu\text{-}I)]_4O_4$ (**2′**). Complex **2** undergoes an effective oxo-transfer reaction converting PPh_3 into $O{=}PPh_3$ under anaerobic conditions. At sufficiently high concentration of PPh_3, the oxygen atom transfer from **2** to PPh_3 was followed by the formation of $[Cu(PPh_3)_3I]$. The dioxygen reactivity of **1** was compared with that known for other halo(amine)copper(I) dimers.

Introduction

Complexes formed between copper(I) halides and amines are the source for various practical catalytic systems that utilize dioxygen as the formal oxidant.[1] Owing to the high affinity of copper(I) halide complexes for polyamines, a large diversity of halo(amine)dicopper(I) complexes have been synthesized and structurally characterized.[2]

Davies and co-workers[1–6] have studied the stoichiometry, products and kinetics of the oxidation of dimeric copper(I) complexes $[LCuX]_2$ (X = Cl, Br or I, L = peralkylated diamines) by dioxygen. It has been shown that most of the dimeric halo(amine)copper(I) complexes are oxygen sensitive and readily react with dioxygen to generate the corresponding copper(II) dioxygen products with the primary stoichiometry: $2L_2Cu_2X_2 + O_2 \rightarrow 2L_2Cu_2X_2O$. The oxidation of $[LCuX]_2$ dimers is characteristically a third-order reaction for X = Cl, Br,[3,4] but second-order for X = I.[5]

Temperature is an important factor governing the extent of dioxygen reduction by these dicopper(I) complexes in aprotic solvents.[2] The chloro and bromo derivatives completely reduce dioxygen at temperatures ≥247 K to give the green dimeric oxocopper(II) complex $[LCuX]_2O$ (**C**). However, at lower temperatures (≤233 K), two tetranuclear mixed-valence (peroxodicopper(I,II))$_2$ intermediates (**A** and **B**) have been reported (Scheme 1). These species, which exist in equilibrium, are stable at low temperatures, but decompose irreversibly to the green oxocopper(II) complex (**C**), according to the reaction **A** → **2C** (Scheme 1).[4,6] The tetranuclear mixed-valence (peroxodicopper(I,II))$_2$ complex $[(DEED)CuBr]_4O_2$ has a half-life of 3.2 h at 298 K.[6] In comparison, the half-life for $[LCuCl]_2O_2$ is 25 s over the temperature range 234–241 K.

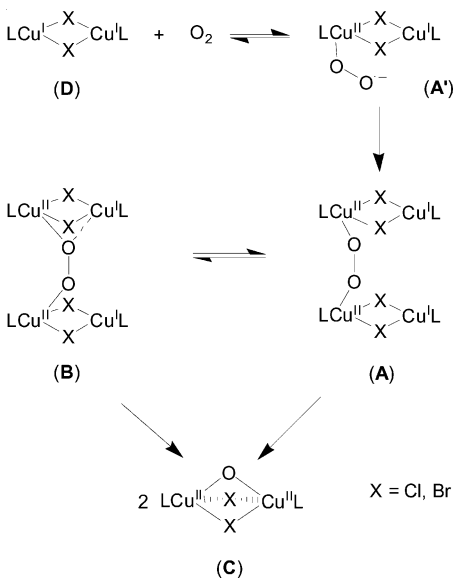

Scheme 1

[a]*Institute of Chemistry, Academia Sinica, Taipei, 115, Taiwan E-mail: chans@chem.sinica.edu.tw; Fax: 886-2-2789-8654; Tel: 886-2-2789-8654*
[b]*Department of Chemistry, The Chinese University of Hong Kong, Shatin, New Territories, Hong Kong SAR. E-mail: hklee@cuhk.edu.hk; Fax: 852-2603-5057; Tel: 852-2609-6331*

† Electronic supplementary information (ESI) available: Fig. S1, Fig. S2 and Table S1. See DOI: 10.1039/b513898a

It is noteworthy that the reactivity of the dimeric complexes toward dioxygen increases as the halide ligand is changed from chloride through bromide to iodide. With the iodo derivatives, no dinuclear peroxodicopper(I,II) or the tetranuclear (peroxodicopper(I,II))$_2$ complexes have been observed. Instead, oxygenation of [LCuI]$_2$ led to the formation of an oxocopper(II) product [LCuI]$_2$O according to the equation [LCuI]$_2$ + O$_2$ → 2[LCuI]$_2$O.[5] Nevertheless, it has been assumed that the reaction of [LCuI]$_2$ with dioxygen proceeds *via* the formation of a peroxodicopper(II) intermediate [LCuI]$_2$(O$_2$), with this step being rate-determining.[5]

We report herein the synthesis, structure and dioxygen reactivity of [Cu(L)(μ-I)]$_2$ (**1**), a bis(μ-iodo)dicopper(I) complex supported by the ligand [*N*-(3,5-di-*tert*-butyl-2-hydroxybenzyl)-*N*,*N*-di-(2-pyridylmethyl)]amine (L) (Chart 1). To date, studies have focused on dimeric halo(amine) dicopper(I) complexes supported by simple peralkylated diamine ligands, and there has been a paucity of data on the dioxygen reactivity of dimeric halo(amine)dicopper(I) complexes supported by ligands with potential N,O-donor sites. In this work, we have studied the oxygenation of **1** in dichloromethane solutions at the temperature range of 193 to 298 K, and examined the structure of the putative copper–dioxygen adduct [Cu(L)(I)]$_2$O$_2$ (**2**) using UV-vis, EPR, NMR, Cu X-ray absorption spectroscopy, and mass spectrometry. Specifically, the structures of the peroxodicopper(II) species have been characterized, and their abilities to effect the oxygen atom transfer reactions toward exogenous substrates have been delineated by examining the corresponding oxygen-atom-transfer reaction(s) to PPh$_3$.

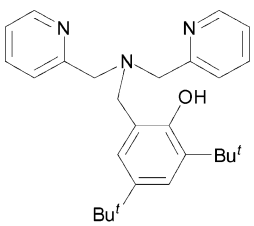

L

Chart 1

Results

Synthesis of [Cu(L)(μ-I)]$_2$ (1)

The bis(μ-iodo)dicopper(I) complex **1** (Fig. 1) was readily prepared by treating a slurry of copper(I) iodide in anhydrous THF with [*N*-(3,5-di-*tert*-butyl-2-hydroxybenzyl)-*N*,*N*-di-(2-pyridylmethyl)]amine (L) in the presence of triethylamine (Scheme 2). It was isolated as a yellow microcrystalline solid in good yield. As the complex was extremely sensitive to air, it was necessary to handle the experimental procedures under a purified nitrogen atmosphere. In our hands, the complex was soluble in polar organic solvents such as dichloromethane and THF, but less soluble in toluene.

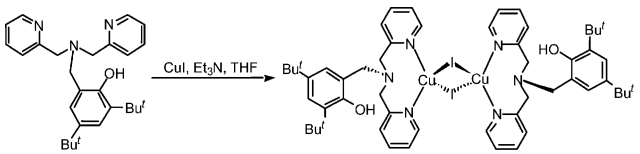

1 80%

Scheme 2

The electronic spectrum of **1** (see Fig. 3(a) later) showed an absorption band at λ_{max} = 318 nm at 193 K; there were no absorptions noted in the 350–900 nm region (*vide infra*). Both spectroscopic and combustion data were consistent with the molecular formula of **1** as determined by X-ray crystallography.

The role of triethylamine in the synthesis of **1** requires comment. The phenolic group of L was not deprotonated by triethylamine. However, the presence of the base was important to afford a clean reaction and facilitate the crystallization of **1**.‡ Attempts to deprotonate the phenol pendant using stronger bases such as sodium hydroxide or *n*-butyllithium only yielded a deep reddish-brown intractable oil. Attempts to prepare other dicopper(I) complexes by reacting L with [Cu(CH$_3$CN)$_4$](PF)$_6$ or [Cu(CH$_3$CN)$_4$](ClO$_4$) were also unsuccessful. This may be ascribed to a high stability constant of the [Cu(CH$_3$CN)$_4$]$^+$ complexes.

Crystal structure of [Cu(L)(μ-I)]$_2$·2CH$_2$Cl$_2$

Single crystals of **1**·2CH$_2$Cl$_2$ were obtained from a dichloromethane solution. Fig. 1 shows the molecular structure of **1**·2CH$_2$Cl$_2$ as determined by single-crystal X-ray crystallography. Crystal data, and selected bond distances (Å) and angles (°) for the complex are summarized in Table 1 and Table 2, respectively. Complex **1** crystallized as a symmetrical copper dimer with the two Cu(I) centers connected by two Cu–(μ-I)–Cu bridges, forming a Cu$_2$I$_2$ core. The complex assumed an idealized C_2 molecular symmetry with a two-fold axis passing through the two iodide ligands. Each Cu(I) center is bonded to two pyridyl nitrogens of a L ligand and two bridging iodide ions, resulting in a distorted tetrahedral N_2I_2 coordination geometry. The observed Cu–N(pyridyl) bond distances are 2.060(3) and 2.062(3) Å, whereas the Cu–I distances are 2.6161(5) and 2.7826(5) Å. The amino nitrogen atoms [N(3) and N(3A)] do not coordinate to the copper atoms as exemplified by the very long copper–nitrogen distance [Cu(1)···N(3)] of 3.795 Å. On the other hand, intramolecular hydrogen bondings

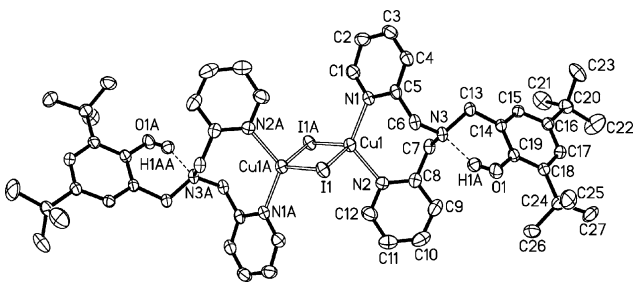

Fig. 1 Molecular structure of [Cu(L)(μ-I)]$_2$·2CH$_2$Cl$_2$ showing the atom labeling scheme. The CH$_2$Cl$_2$ solvate molecules are omitted for clarity.

‡ We have attempted to prepare a copper(I) phenolate complex *via* deprotonation of ligand L with triethylamine. However, the phenol group of L was inert towards the base. When we attempted to prepare **1** in the absence of this base, no pure, crystalline product could be isolated (as revealed by NMR spectroscopy). Conceivably, the presence of triethylamine in the reaction mixture may reduce the formation of other unknown side products, and provide an appropriate condition for crystallization of **1**.

Table 1 Crystallographic data for $[Cu(L)(\mu\text{-}I)]_2 \cdot 2CH_2Cl_2$ (**1**·$2CH_2Cl_2$) and $[Cu(L)Cl]Cl \cdot 2CHCl_3$ (**4**·$2CHCl_3$)

	1·$2CH_2Cl_2$	**4**·$2CHCl_3$
Mol. formula	$(C_{54}H_{70}Cu_2I_2N_6O_2) \cdot 2CH_2Cl_2$	$(C_{27}H_{35}Cl_2CuN_3O) \cdot 2CHCl_3$
Mol. weight	1385.9	790.76
Crystal size/mm^3	0.71 × 0.65 × 0.54	0.15 × 0.12 × 0.08
Crystal system	Monoclinic	Monoclinic
Space group	$C2/c$	$P2_1/n$
a/Å	38.658(2)	11.6412(3)
b/Å	9.2999(5)	18.7028(5)
c/Å	18.7382(10)	16.4521(4)
α/°	90	90.00
β/°	110.7820(10)	95.529(2)
γ/°	90	90.00
Z	4	4
V/Å^3	6298.4(6)	3565.34(16)
T/K	293(2)	100(2)
Density/g cm^{-3}	1.462	1.473
Abs. coefficient/mm^{-1}	1.867	1.240
Reflection collected	21414	26772
Unique data measured	7588 ($R_{int} = 0.0233$)	6299 ($R_{int} = 0.0596$)
Obs. data with $I \geq 2\sigma(I)$	5751	3995
No. of variable	327	383
Final R indices [$I \geq 2\sigma(I)$][a]	$R1 = 0.0385$	0.0305
	$wR2 = 0.1002$	0.0491
R indices (all data)[a]	$R1 = 0.0537$	0.0544
	$wR2 = 0.1057$	0.0510

[a] $R1 = \sum \| F_o | - | F_c \| / \sum | F_o |$; $wR2 = \{\sum[w(F_o^2 - F_c^2)^2] / \sum[w(F_o^2)^2]\}^{1/2}$.

Table 2 Selected bond distances (Å) and angles (°) for $[Cu(L)(\mu\text{-}L)]_2$ (**1**)

Cu(1)···Cu(1A)	2.9106(8)
Cu(1)–I(1)	2.7826(5)
Cu(1)–N(1)	2.062(3)
Cu(1)–I(1A)	2.6161(5)
Cu(1)–N(2)	2.060(3)
Cu(1)–I(1)–Cu(1A)	65.16(2)
I(1)–Cu(1)–I(1A)	114.84(2)
N(1)–Cu(1)–N(2)	119.1(1)
N(1)–Cu(1)–I(1)	106.41(7)
N(1)–Cu(1)–I(1A)	110.52(8)
N(2)–Cu(1)–I(1)	97.45(8)
N(2)–Cu(1)–I(1A)	108.19(8)
N(1)–Cu(1)–Cu(1A)	125.81(7)
N(2)–Cu(1)–Cu(1A)	113.86(8)

between the phenolic protons and the amino nitrogen atoms (H1A···N3 1.961 Å) were observed. The Cu···Cu separation was determined to be 2.9106(8) Å.

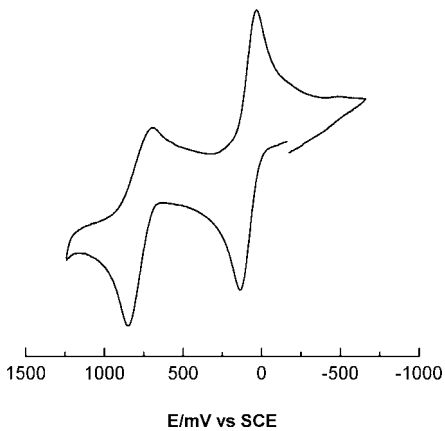

Fig. 2 Cyclic voltammogram of complex **1** in CH_2Cl_2 containing 0.12 M of $[^nBu_4N][PF_6]$ at a scan rate of 100 mV s^{-1}.

Electrochemistry

The electrochemical behavior of **1** was studied by cyclic voltammetry (Fig. 2). All potentials were measured in dichloromethane with tetrabutylammonium hexafluorophosphate as the supporting electrolyte and internally referenced to the ferrocenium/ferrocene redox couple. Potentials were reported *versus* SCE with $E_{1/2}$ for the Fc^+/Fc couple = 0.435 V in $CH_2Cl_2/[^nBu_4N][PF_6]$.[7]

The cyclic voltammogram of **1** consists of a reversible oxidation peak at $E_{1/2}$ = 86 mV (ΔE = 108 mV, i_a/i_c = 1.0) and a quasi-reversible peak at $E_{1/2}$ = 772 mV (ΔE = 158 mV, i_a/i_c = 1.4), which may be ascribed to the $[Cu(L)(\mu\text{-}I)]_2^+/[Cu(L)(\mu\text{-}I)]_2$ and $[Cu(L)(\mu\text{-}I)]_2^{2+}/[Cu(L)(\mu\text{-}I)]_2^+$ couples, respectively. Interestingly, the mean reduction potential for the two Cu(II) centers in complex **1** is substantially lower than those of other dicopper(I) complexes reported in the literature.[7–9] However, there is a strong anti-cooperative redox interaction between the two copper centers in **1** when the system is oxidized/reduced. It is established that T_d is not a favorable coordination geometry for Cu(II). Accordingly, there must be a substantial structural rearrangement of the complex required to attain the coordination number and geometry preferred for the copper ions when they are both oxidized. Consistent with this, the oxidation wave at 772 mV exhibited much less electrochemical reversibility than the wave at 86 mV.

Dioxygen reactivity of $[Cu(L)(\mu\text{-}I)]_2$ in CH_2Cl_2

We have investigated the reactivity of complex **1** towards dioxygen in some detail. These experiments were conducted under an otherwise purified inert atmosphere. Bubbling dioxygen through

a solution of **1** in CH_2Cl_2 at 193 K induced a color change, first to slightly purple and then deep green.§ The corresponding UV-vis spectrum of the final product (Fig. 3(b)) consisted of pronounced, broad absorption bands in the range of 300–350 nm with a poorly defined absorption maximum at ~330 nm (ε, 6400 ± 180 $dm^3\ mol^{-1}\ cm^{-1}$ per dicopper complex), two intense charge-transfer bands at 410 nm (4100 ± 100) and 576 nm (2250 ± 70), a shoulder peak at ~456 nm, and, presumably, a d–d transition at 670 ± 10 nm (950 ± 20). An isosbestic point was observed at 292 nm, suggesting that only two principal species, namely complex **1** and its oxygenated species **2**, were present in the oxygenated solution at low temperatures (Fig. 3 inset).

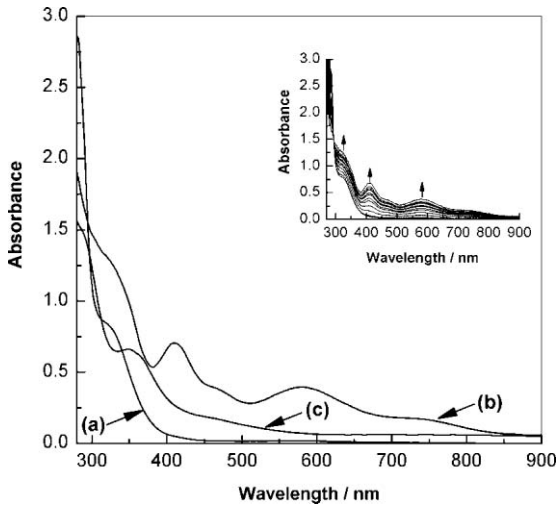

Fig. 3 Optical absorption spectra of (a) complex **1** in CH_2Cl_2, (b) the copper-dioxygen species **2** generated at 193 K in CH_2Cl_2, and (c) the brown solution obtained upon decomposition of **2** at room temperature. Inset: development of optical absorption spectra upon oxygenation of **1** in CH_2Cl_2 at 193 K.

Mild warming of an oxygenated solution of **1** to 203 K, or purging the oxygenated solution with a stream of argon gas at 193 K resulted in no noticeable loss/change in absorption intensity of the UV-Vis spectra of the solutions. Thus, the oxygenation of **1** was irreversible. Although the oxygenated species **2** was rather stable at low temperatures, it slowly decomposed at room temperature, as evidenced by fading of the green color of the oxygenated solution within one day and the concomitant appearance of new absorption bands in the UV-vis spectrum (Fig. 3(c)).

§ We assigned the purple color species to the mixed-valence intermediate complex shown in Scheme 3. Consistent with this assignment, no purple color was observed upon oxygenation of **1** at higher temperatures, at which the reaction rate was much higher. Unfortunately, we were unable to obtain the optical absorption spectrum of this intermediate species. It is believed that both the intermediate species and complex **2** may have comparable absorption bands, albeit different extinction coefficients. This scenario is likely to be the case if we compare the absorption features of **2** with those of other transient superoxocopper(II) species reported in the literature. The optical absorption spectrum of **2** consists of an intense CT absorption at 410 nm (ε, 4100 ± 100 $dm^3\ mol^{-1}\ cm^{-1}$) and, presumably, a d–d transition at 670 nm (950 ± 20). These values are comparable to those reported for most transient superoxocopper(II) species, which consist of an intense CT absorption band at 410 nm (ε, 3000–8000 $dm^3\ mol^{-1}\ cm^{-1}$), and two weaker features at ~600 nm (1000–1700) and 750 nm (1000), respectively.[10]

The effects of temperature on the optical absorption spectrum of the oxygenated species **2** were also studied over a greater temperature range. Upon warming an oxygenated solution of **1** from 193 K to 243 K and to 263 K, only minor changes were noted in the intensity of the absorption bands in the visible region (Fig. 4). There was a small red shift of the peaks at 410 nm, 456 nm and decrease in the absorbance in the range of 300–340 nm in the near-UV region. Further increase of the temperature to 273 and 283 K resulted in a pronounced absorption at 334 nm. Warming of a sample of **2** from 193 K to 263 K followed by subsequent cooling of the solution back to 193 K regenerated the original spectrum, including blue shift of the peaks at 410, 456 nm and almost full recovery of the absorbance in the range of 300–340 nm (Fig. 4 inset). Irreversible spectral changes were only observed when the solution was warmed further to 283–293 K. Thus, the oxygenated species **2** was stable up to 263 K, although it appeared that there were two similar species in equilibrium occurring between 193 K and 273 K. The changes in the electronic spectra of species **2** are more easily observed from the deconvolution of its spectra generated at different temperatures (Fig. S1, ESI).†

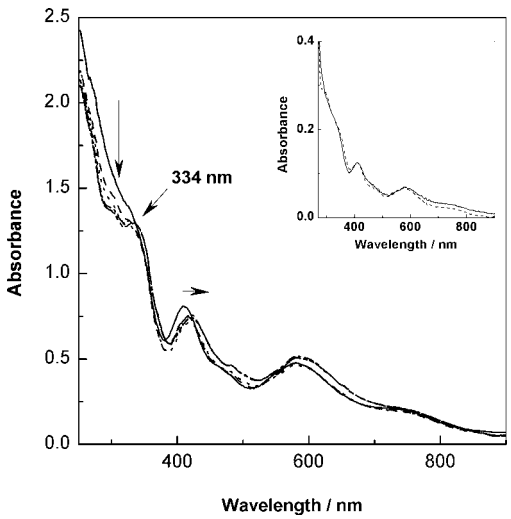

Fig. 4 Optical absorption spectra measured upon warming a solution of **2** in CH_2Cl_2 from 193 K to 283 K. Inset: optical absorption spectra measured for oxygenation of **1** in CH_2Cl_2 at 193 K (solid line), followed by warming the solution to 263 K and subsequent cooling of the solution back to 193 K (dashed line).

The absorption of **2** at ~334 nm may be ascribed to an $O_2^{2-} \rightarrow$ Cu(II) CT transition.[4,10] Since species **2** catalyzes the quantitative conversion of PPh_3 to $O{=}PPh_3$ under anaerobic conditions (*vide infra*), we surmise that the reaction of **1** with dioxygen has produced a copper–dioxygen adduct with a highly covalent Cu–O bond.

The electronic spectra of **2** at low temperatures are comparable with those of the related oxygenated species $[Cu(L')(\mu\text{-}X)]_2O$ and $[Cu(L')(\mu\text{-}X)]_2O_2$ (X = Cl, Br, I; L′ = peralkylated diamines).[3–6] The transition energies at 410, 456 and 576 nm of **2** are close to those observed at 435 and 600–650 nm for the related iodo-oxocopper(II) dimer $[Cu(L')(\mu\text{-}I)]_2O$,[5] though the molar absorptivities for **2** are 4- to 5-fold higher. On the other hand, the energy and intensity of the transition at 334 nm (ε, 6400 $dm^3\ mol^{-1}\ cm^{-1}$) for complex **2** resemble the bands at 320–380 nm previously reported for the peroxodicopper(II) species $[(TEED)CuX]_2O_2$ (X = Br, Cl).[4,6]

A comparison of the electronic spectrum of **2** with those of other copper–dioxygen model complexes[10–17] supports the formation of a dicopper(II)-peroxo species since the energy and intensity of the CT transition for **2** are close to those observed for other dicopper(II)-peroxo complexes. In particular, the energy and intensity of the CT transition in **2** are closer to those of the μ-1,1-hydroperoxo-bridged binuclear Cu(II) complex previously described for the peroxide intermediate of laccase [λ_{max}/nm 340 (ε, 5000 dm^3 mol^{-1} cm^{-1}), 470 (1800); and weak band at 670][11] as well as for other dicopper(II) hydroperoxo complexes [λ_{max}/nm 370 (ε, 3700 dm^3 mol^{-1} cm^{-1}); and broad band at 650 (300)] reported by Karlin *et al.*[12] and Teramae and co-workers.[13]

Thus, we conclude that **1** binds one dioxygen molecule to form a peroxodicopper(II) complex **2**. The strong absorptions in the region of 300–340 nm and 580 nm are assigned, respectively, to the O_2^{2-} (π_σ*) → Cu^{II} and O_2^{2-} (π_v*) → Cu^{II} CT transitions of **2**, in accordance with previous assignments of analogous transitions in other peroxodicopper(II) complexes.[11,14,15]

The lower intensity of the π^*_σ CT transition of **2** relative to those observed for other side-on μ-η^2:η^2-peroxodicopper(II) or end-on *trans* μ-1,2-peroxodicopper(II) complexes could be accounted for by the presence of the iodo bridges between the two Cu(II) centers in **2**. Consequently, the peroxide moiety in **2** has less σ-donor interaction with the copper atoms than in the case of other side-on and *trans* end-on dimers.[11]

The strong absorption at 410 nm could be assigned to a iodide–Cu(II) CT transition.[5,18,19] No absorptions characteristic of free iodine or tri-iodide[20] were observed, indicating that the iodide ligands in **1** were not oxidized and released during the reaction of the complex with dioxygen.

Release of hydrogen peroxide when 2 is treated with acid

The formation of a peroxodicopper(II) complex from the reaction of [Cu(L)(μ-I)]$_2$ with dioxygen at low temperatures was corroborated further by the Ampex Red reagent test for hydrogen peroxide. In a typical experiment, a solution of **2** in CH_2Cl_2 was cooled to 193 K, followed by treatment with excess HBF_4/Et_2O. A small amount of the acidified solution was added to an aqueous sodium phosphate buffer (pH = 7.4) containing the Ampex Red reagent and horseradish peroxidase. The solution was incubated for 15 min and the fluorescence spectrum (540–700 nm with excitation at 530 nm) recorded using a steady-state spectrofluorometer (Fig. 5). The characteristic emission at λ = 585 nm indicated the presence of resofurin, an oxidation product due to the reaction of Ampex Red with H_2O_2 in the presence of peroxidase. A quantitative study showed that 88% of the oxygen associated with the oxygenated species was recovered as H_2O_2 upon treatment of **2** with acid (an average of 3 assays). This result is consistent with a 1 : 1 stoichiometry for the dioxygen adduct of **1**.

The quantity of H_2O_2 obtained from the acid treatment of **2** was also determined by iodometry. This method gave a yield of ~85% (an average of 5 determinations), again consistent with the 1 : 1 stoichiometry in **2**.

Changes in the electronic spectrum confirmed that protonation of the peroxo-species **2** in the presence of strong acid at low temperatures releases H_2O_2 (Fig. 6). Karlin and co-workers have reported similar observations upon treating a *trans* end-on, phenoxo-bridged peroxodicopper(II) species with a strong

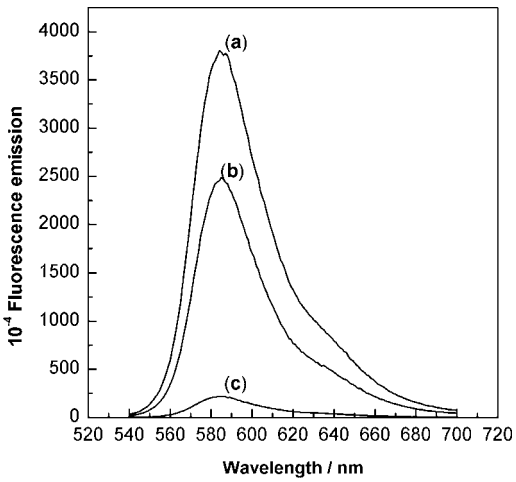

Fig. 5 Fluorescence emission spectra of resorufin generated by reacting Ampex Red (in the presence of peroxidase) with (a) a standard solution of H_2O_2, (b) an experimental solution, and (c) a control reaction without H_2O_2; λ_{ext} = 530 nm.

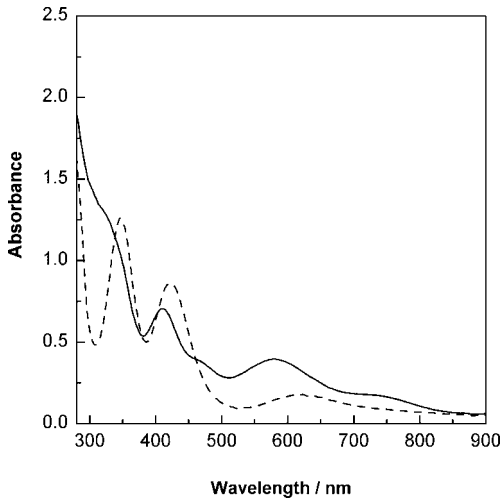

Fig. 6 Optical absorption spectra of **2** obtained upon oxygenation of **1** in CH_2Cl_2 at 193 K (solid line), followed by addition of excess HBF_4/Et_2O at 193 K (dashed line).

acid.[12] The peroxo group in the copper–dioxygen complex under study reacts similarly, a characteristic of basic/nucleophilic M$_n$–O_2 compounds.

Cu *K*-edge absorption spectroscopy

Cu *K*-edge absorption spectroscopy was used to ascertain the oxidation state of copper ions in complex **2**. Fig. 7 depicts the Cu *K*-edge absorption spectrum of **2**. A weak pre-edge feature centered at 8978.4 eV was observed, corresponding to the 1s → 3d transition for Cu(II). The specific transitions at 8987.1 and 8993.2 eV are assignable to the 1s → 4p + LMCT shakedown and 1s → 4p transitions, respectively.[21] These spectral features are more easily discerned in the second derivative spectrum (see inset of Fig. 7), where the peaks become enhanced against the background. The Cu *K*-edge XAS spectrum indicates that **2** is indeed a peroxodicopper(II) species.

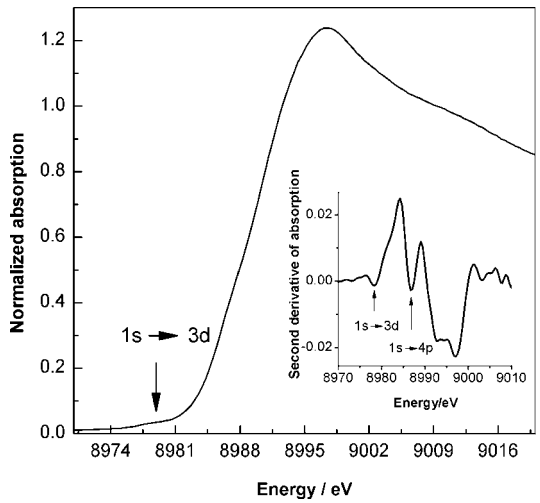

Fig. 7 Cu *K*-edge X-ray absorption spectrum of **2** and its second derivative spectrum (inset) recorded at 77 K. Species **2** was generated upon oxygenation of **1** in CH_2Cl_2 at 193 K.

Mass spectrometry analysis

In order to identify the chemical species present in solutions of the oxygenated species **2** at ~233 K as well as at room temperature, a solution of complex **1** in CH_2Cl_2 oxygenated at 193 K was warmed up to the two temperatures, and aliquots were injected into a Finnigan LCQ or QSTAR Pulsari mass spectrometer equipped with a Q-TOF analyzer for electrospray ionization (ESI) mass analysis. The spectra revealed positive ion clusters at *m*/*z* 1729, 1250 and 1243 (small), 995, 977 and 515 corresponding to the $\{[Cu_3(L)_3I_2O_2] + H]\}^+$, $\{[Cu_2(L)_2I_2O_2] + 2H]\}^+$, $\{[Cu_2(L)_2I_2O_2] - 2H\}^+$, $\{[Cu_2(L)_2O_2] + H\}^+$, $\{[Cu_2(L)_2O] - H\}^+$ and $\{[Cu(L)OOH] + 2H\}^+$ fragments (Fig. 8, 9). In addition, positive ion clusters were detected at *m*/*z* 1821, 1693, 1215, 1087, 607, 479. The latter mass values and their distribution isotope patterns are consistent with a $\{[Cu_3(L)_3I_3] - 2H\}^+$, $\{[Cu_3(L)_3I_2] - 3H\}^+$, $\{[Cu_2(L)_2I_2] - H\}^+$, $\{[Cu_2(L)_2I] - 2H\}^+$, $[Cu(L)I]^+$, $[Cu(L) - H]^+$ ion fragments, respectively (Fig. S2, ESI).† From these data, it was evident that the iodides were not displaced during the reaction of **1** with dioxygen. Additionally, positive ion clusters at 2337,

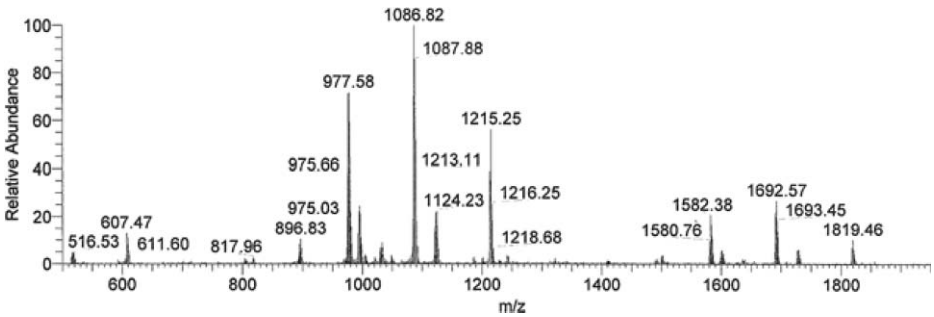

Fig. 8 ESI-MS of **2** in CH_2Cl_2.

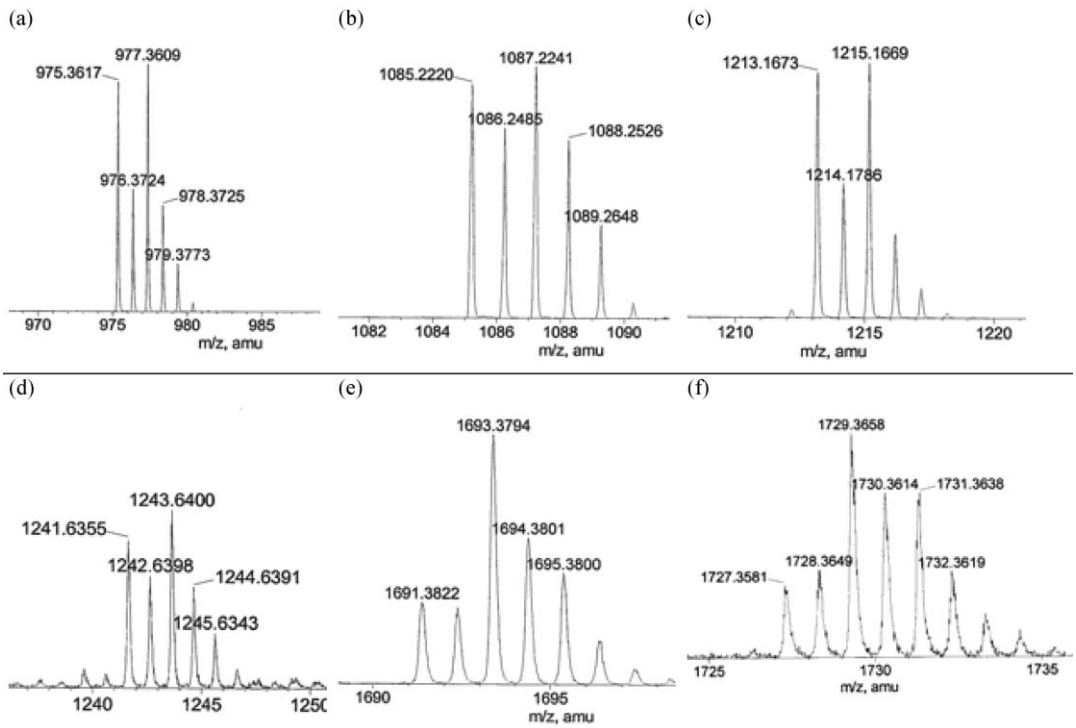

Fig. 9 Sections of a TOF-MS of **2** in CH_2Cl_2 showing the distribution isotope patterns for positive ion clusters of (a) $\{[Cu_2(L)_2O] - H\}^+$, (b) $\{[Cu_2(L)_2I] - 2H\}^+$, (c) $\{[Cu_2(L)_2I_2] - H\}^+$, (d) $\{[Cu_2(L)_2I_2O_2] - 2H\}^+$, (e) $\{[Cu_3(L)_3I_2] - 3H\}^+$, and (f) $\{[Cu_3(L)_3I_2O_2] + H]\}^+$.

2302, 2247, 2209 (with not well resolved distribution isotope pattern) were observed, corresponding to the $\{[Cu_4(L)_4I_3O_2] + H\}^+$, $\{[Cu_4(L)_4I_3] - 2H\}^+$, $[Cu_4(L)_4I_3]^+$ and $[Cu_4(L)_4I_2O_2]^+$ ion fragments, respectively. These mass peaks provide evidence of a tetranuclear (peroxodicopper(II))$_2$ species, suggesting that the bis(μ-iodo)peroxodicopper(II) **2** may exist as a dimer, and perhaps, there exists an equilibrium between dinuclear peroxodicopper(II) complex **2** (or dimer) and the tetranuclear (peroxodicopper(II))$_2$ **2′** (or tetramer) according to Scheme 3. Although the parent ion corresponding to $[Cu_4(L)_4I_4O_4]^+$ has not been observed, the fragmentation patterns observed are certainly consistent with this scenario. Interestingly, the most abundant ion cluster was observed at m/z 1087, indicating that the $[Cu_2(L_2)I]^+$ dimer was the most stable ion fragment.

EPR spectroscopy

Fig. 10(a) and (b) show the 4 K EPR spectra of the green species **2** recorded for two preparations obtained by the reaction of **1** with O_2 in CH_2Cl_2 at 193 K. These EPR spectra appear complex, but from the splittings of the hyperfine components observed at the lower-field edge and the overall width of the spectrum, we surmise that it is a superposition of spectra from different type 2 centers with a distribution of $g_{//}$, $g_{\perp}$, $A_{//}$, and $A_{\perp}$ values, each spectral broadened by electron–electron dipolar interactions with one or more other type 2 centers. Such a spectrum would be obtained for a dinuclear peroxodicopper(II) species, or a tetranuclear (peroxodicopper(II))$_2$ species, if only Zeeman interactions, hyperfine interactions and magnetic dipolar interactions contribute to the spin Hamiltonian. In other words, the pairwise electronic exchange interactions among the Cu(II) centers within each of these complexes are negligible. Given that the Cu(II) centers in the peroxodicopper(II) complex are bridged by large iodide anions that do not mediate spin polarization effectively, and the Cu(II)$\cdots$Cu(II) distance is at least 2.9 Å, this scenario is likely to be the case. In case of the tetranuclear (peroxodicopper(II))$_2$ species, each Cu(II) center should also be linked to another *via* a peroxide bridge, where the Cu(II)$\cdots$Cu(II) distances are even longer across the dimeric units that form the tetranuclear complex. However, for this species, there might be weak antiferromagnetic interactions across the dimeric units mediated by the bridging peroxides (*vide infra*). In any case, we expect the EPR spectrum for each paramagnetic species to be merely a sum of contributions from the different mononuclear type 2 Cu(II) sites within each complex amended by the dipolar interactions among the Cu(II) centers. Depending on the magnitude of the magnetic dipolar interactions, the overall spectral width as measured at the base line should increase the larger the interactions, and the overall spectrum should become increasingly symmetrical and centered at $g_{average}$. The positions of $g_{//}$, $g_{\perp}$ values for a type 2 Cu(II) center are highlighted in the EPR spectrum, as well as the position of $g_{average}$, and from the appearance of the overall spectrum, it is evident that this is indeed the case.

Finally, since the observed spectrum should also be a superposition of spectra from a number of species, *e.g.*, copper(II) dimers and tetramers, the actual EPR spectrum should reflect the distribution of species within a given sample depending on the details of the preparation as well as the temperature from which the sample was quickly frozen for the low temperature EPR measurements.

In support of the above interpretation, we have also recorded the EPR spectra of the green species **2** at 4, 40 and 77 K under various microwave powers. The data obtained at 4 K are shown in Fig. 11. As expected, the EPR spectrum saturated uniformly with increasing microwave power, and there was gradual total loss of the Cu(II) hyperfine structure without significant distortion of the overall shape, with the apparent overall line width remaining almost unchanged.

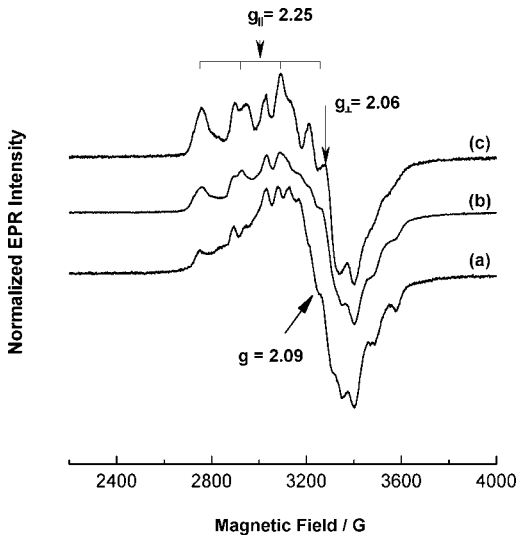

Fig. 10 Comparison of the 4 K EPR spectra for the copper–dioxygen species **2**, generated by oxygenation of **1** in CH_2Cl_2 at 193 K (a, b) and 283 K (c).

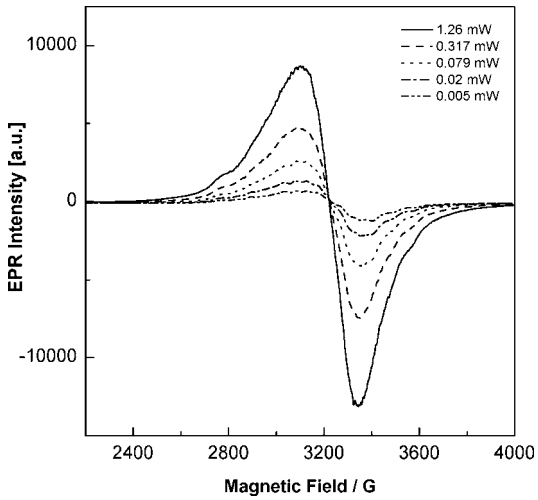

Fig. 11 4 K EPR spectra of **2** recorded under various microwave powers. Species **2** was generated upon oxygenation of **1** in CH_2Cl_2 at 193 K.

Integration of the EPR spectra under low microwave powers (0.005–0.02 mW) at 4 K, 40 K and 77 K, revealed that the EPR intensity accounted for only 60% of the copper ions in the sample. Thus, it is evident that some of the copper ions in the solution are associated with complexes that are diamagnetic and EPR silent. Since the EPR intensity was found to be essentially independent of temperature, these diamagnetic or EPR silent copper species are evidently not in dynamic equilibrium with the green species **2**. The equilibrium between the dinuclear peroxodicopper(II) species and

the tetranuclear (peroxodicopper(II))$_2$ species for the oxygenated complex **2** would not contribute a temperature dependence to the EPR intensity if the antiferromagnetic interactions across the dimeric units mediated by the bridging peroxides in the tetranuclear (peroxodicopper(II))$_2$ species are sufficiently weak.

Reaction of complex 2 with PPh_3

The reactivity of **2** toward PPh_3 was examined under both limiting dioxygen (anaerobic) and excess dioxygen (aerobic) conditions, at different temperatures and at different ratios of the precursor $[Cu(L)(\mu\text{-}I)]_2$ to PPh_3. As summarized in Table 3, complex **2** is an effective oxo-transfer agent for complete conversion of PPh_3 into $O{=}PPh_3$ either under anaerobic or aerobic conditions.

The stoichiometry of the reaction of **2** with PPh_3 was determined by using different molar ratios of the precursor $[Cu(L)(\mu\text{-}I)]_2$ to PPh_3 followed by quantitative product analysis by GC-MS and by $^{31}P\{^1H\}$NMR spectroscopy. On the basis of integration against an internal standard in the GC-MS, the ratio of $O{=}PPh_3/PPh_3$ was determined to be 1 : 1, 1 : 1 and 1 : 2 for ratios of $\{[Cu(L)(\mu\text{-}I)]_2\}_0/[PPh_3]_0$ equal 1 : 1, 1 : 2 and 1 : 3, respectively, with a 87% recovery of the products based on the amounts of PPh_3 added, and a $O{=}PPh_3$ yield of 98% based on the quantity of $[Cu(L)(\mu\text{-}I)]_2$ complex used for the reaction. Thus, the stoichiometry of the process was 1 : 1 with respect to complex **1** and PPh_3; in other words, only one oxygen atom was transferred from **2** to PPh_3.

The reaction between complex **2** and triphenylphosphine was also followed spectrophotometrically by the intensity decrease of the characteristic absorbance at 334, 410 and 576 nm due to complex **2** in CH_2Cl_2 at low temperatures (193 K) under anaerobic conditions. When the reaction was carried out at low temperatures ≤243 K only small changes in the absorbance were observed. At ambient temperatures, the spectral changes were more pronounced. Accordingly, the kinetics of the reaction was followed at 288 K.

The reaction between **2** and PPh_3 is complex. It obeyed first-order kinetics over the first 20 min (Fig. 12) in the presence of an excess amount of the PPh_3 under anaerobic conditions. A rate constant could be determined from the initial rate over the first 500 s (Fig. 12, inset). A plot of the pseudo first-order rate constant k_{obs} against the initial concentration of triphenylphosphine under anaerobic conditions provided a straight line: $y = 0.12x + (2 \times 10^{-5})$ ($R^2 = 0.9987$) with a nearly zero intercept and a slope from which the pseudo second-order rate constant 1.2×10^{-1} M^{-1} s^{-1} was obtained (Fig. 13).

Table 3 Formation of $O{=}PPh_3$ (%) from the reaction of **2** with PPh_3 under various conditions

Reaction	Temperature/K	Yield of $O{=}PPh_3$ (%)
Condition 1 (aerobic)	243 (18 h)	86
1 + O_2 → **2**	273	91
2 + PPh_3 → $O{=}PPh_3$	293	100
Condition 2 (aerobic)	243 (18 h)	90
1 + PPh_3 → {**1**·PPh_3}	273	100
{**1**·PPh_3} + O_2 → $O{=}PPh_3$	293	100
Condition 3 (anaerobic)	263	97
1 + O_2 → **2**	288	92
2 + PPh_3 → $O{=}PPh_3$	273	100

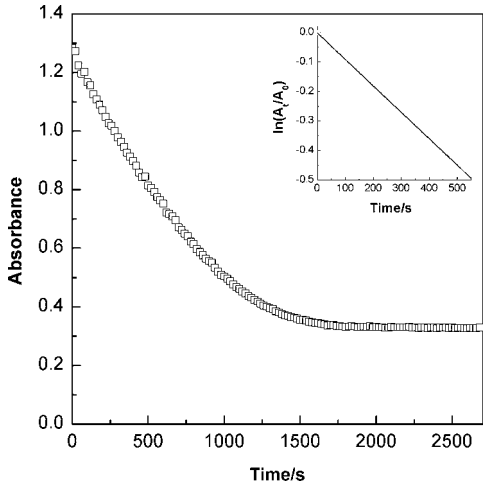

Fig. 12 Kinetic traces for the reaction of **2** with PPh_3 at 288 K recorded by following the absorbance change at 334 nm.

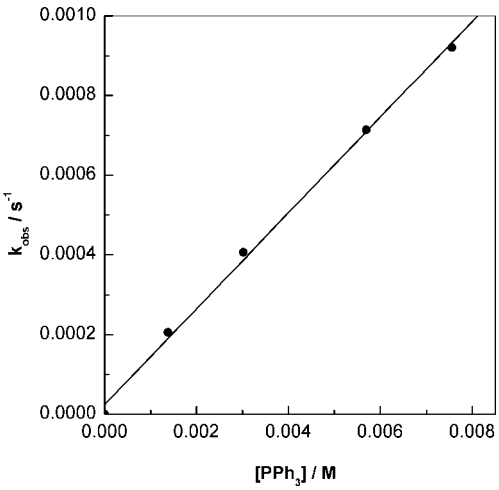

Fig. 13 Plot of pseudo-first order rate constant k_{obs} *vs.* $[PPh_3]_0$ for the reaction of **2** with PPh_3.

We found that the ultimate course of the reaction depended on the ratio of PPh_3 to $[\mathbf{2}]_0$. For molar ratios of $[PPh_3]/[\mathbf{2}]_0 \leq 10$, the solution remained green even after **2** has been consumed, as evidenced by the disappearance of the charge transfer band at 334 nm. On the other hand, if $[PPh_3]/[\mathbf{2}]_0 \geq 10$, the solution quickly turned slightly yellow, with no absorption features remaining in the visible region. The solution was EPR silent and ^1H NMR revealed only sharp resonances with chemical shifts in the 0–10 ppm region, indicating that only diamagnetic species were present in the solution. The diamagnetic complex $[Cu(PPh_3)_3I]$ (**3**) was subsequently isolated from the experimental mixture. Thus the reaction of **2** with excess of PPh_3 was complex and included several consecutive reactions: oxygen atom transfer from **2** to PPh_3 followed by the formation of $[Cu(PPh_3)_3I]$ if the concentration of PPh_3 was sufficiently high.

In addition, if the slightly yellow colored solution of $[Cu(PPh_3)_3I]$ was allowed to stand for a few weeks at room temperature in the presence of air in $CHCl_3$, the reaction mixture turned green and yielded green crystals corresponding to the chloro–copper(II) complex [Cu(L)Cl]Cl (**4**), as characterized by

X-ray diffraction (Fig. 14). Complex **4** was produced by the reductive dechlorination of chloroform by copper(I) followed by the formation of a chloro–copper(II) species with a Cu–Cl covalent bond. This process is analogous to the dehalogenation reactions mediated by copper(I) complexes described by Lucchese *et al.*[22] except that in our case the redox process was much slower and took place in the presence of dioxygen.

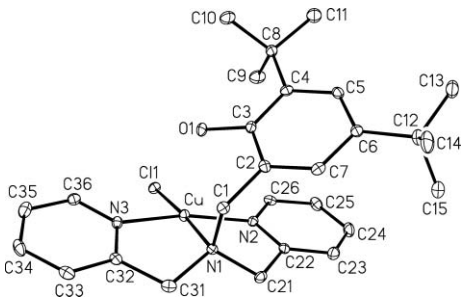

Fig. 14 ORTEP view of $[Cu(L)Cl]^+$ (30% thermal ellipsoids) showing the atom-labelling scheme. Hydrogen atoms, the Cl^- counter anion and the $CHCl_3$ solvate molecules are omitted for clarity.

Discussion

In this study we have prepared and structurally characterized the bis(μ-iodo)dicopper (I) complex **1** supported by a pyridine-containing ligand having a phenol moiety with *t*-butyl substituents. The reactivity of **1** toward dioxygen has been examined at 193 K and above. Complex **1** is oxygen sensitive as are most dimeric halo(amine)copper(I) complexes. But in contrast to the oxygenation of related $[LCuI]_2$ dimers, which generates the oxocopper(II) products $[LCuI]_2O$, the reaction of **1** with dioxygen gives the bis(μ-iodo)peroxodicopper(II) or peroxodicopper(II) complex $[Cu(L)(\mu\text{-}I)]_2O_2$ **2**. Mass-spectrometry data together with low temperature EPR (4 K) have enabled us to deduce that multicopper species exist in the oxygenated solution of **1**, and we have proposed an equilibrium between complex **2** and its dimer, namely, tetranuclear (peroxocopper(II))$_2$ complex **2′**. Thus the use of bulky N_3O-type tripodal ligand as a supporting ligand instead of the simple diamines has led to the stabilization of iodo bridged dinuclear as well as tetranuclear (peroxocopper(II))$_2$ species. X-Ray absorption spectroscopy has established that the peroxodicopper(II) complex and the putative tetranuclear (peroxodicopper(II))$_2$ species are copper(II) complexes in contrary to the mixed valence peroxodicopper(I,II) (**A′**) and tetranuclear (peroxodicopper(I,II))$_2$ species **A** (Scheme 1) suggested for the oxygenation of copper(I) dimers $[LCuX]_2$ (X=Cl, Br).[4,6] On the basis of the experimental results described above, we proposed a scheme for reaction of **1** with dioxygen as shown in Scheme 3. The stoichiometry of the reaction of **1** with dioxygen is 1 : 1 in contrast to the primary stoichiometry of 2 : 1 found for the related dimeric halo(amine)copper(I).[2] Although we have no direct evidence for a η^1-superoxo intermediate, it is possible that the superoxo intermediate is a precursor to the peroxodicopper(II) species **2**, as most experimental data suggest that the oxygenation of copper(I) proceeds through the formation of a Cu(II)-superoxo species.[10]

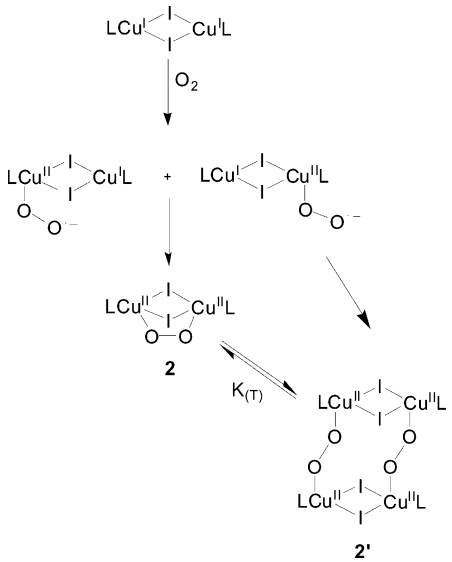

Scheme 3 A proposed scheme for the reaction of $[Cu(L)(\mu\text{-}I)]_2$ with dioxygen.

The peroxo complex **2** exhibits a nucleophilic character similar to that of the end-on peroxodicopper(II) complexes.[16] On the other hand, complex **2** is competent toward stoichiometrically converting PPh_3 into $O{=}PPh_3$, similar to the electrophilic side-on peroxo complexes,[12] but unlike the bis(μ-oxo)dicopper(III) complexes, which have been found to be inert to afford the same oxo-transfer reaction.[23] In one of the bis(μ-oxo)dicopper(III) complexes, supported by *N*,*N*,*N′*,*N′*-tetraethylethylenediamine, the oxygen atom transfer has been shown to be catalyzed by dioxygen, which forms a dioxygen adduct with the bis(μ-oxo)dicopper(III).[23] However, facile oxo-transfer also occurs in the presence of the excess unreacted Cu(I) precursor.[23] These results have implications on the mechanism of the hydroxylation of methane mediated by the putative trinuclear copper clusters in the particulate methane monooxygenase.[24]

Experimental

General procedures

All reactions were carried out under a purified nitrogen atmosphere using modified Schlenk techniques or in a Braun MB 150-M dry-box. Solvents were of reagent grade and dried over and distilled from calcium hydride (CH_2Cl_2), magnesium methoxide (MeOH), or Na/benzophenone (diethyl ether and THF), and degassed either by three freeze–thaw vacuum/purge cycles or by purging with argon for 20 min. The ligand [*N*-(3,5-di-*tert*-butyl-2-hydroxybenzyl)-*N*,*N*-di-(2-pyridylmethyl)]amine (L) was prepared as described previously.[25,26] All reagents were obtained from commercial sources and used as received. Triphenylphosphine (Aldrich) was purified and dried according to published procedure.[27] Ampex Red Hydrogen Peroxide/Peroxidase Assay Kit (A-22188) was purchased from Molecular Probes. Oxygen gas (99.8%) was dried with P_4O_{10} and Drierite, followed by passing through a cold trap (193 K). Oxygen-saturated CH_2Cl_2 was prepared by bubbling oxygen gas through the solvent for 20 min. The solubility of dioxygen in CH_2Cl_2 at 293 K was accepted to be

5.8 mM as reported in the literature.[28,29] The variations in reagent concentration as well as dioxygen solubility in dichloromethane as a function of temperature were calculated by the equations: $d_T = 1.370(2) - 0.00180(2)T$ (T in °C) and $C_T = C_{20\,°C}\,(d_T/d_{20\,°C})$.[29]

Physical methods

GC analysis was performed on a Hewlett-Packard 6890 series gas chromatograph equipped with a capillary injector, a flame ionization detector, and a 50-m HP-1 capillary column. GC-MS analysis was carried out on a Hewlett Packard GC(HP 6890)-MS(HP 5973) analyzer equipped with a HP–5MS (5% phenyl methyl siloxane) column. ^{1}H, ^{13}C{1H} and ^{31}P{^{1}H} NMR spectra were recorded on a Bruker DPX 300 spectrometer (^{1}H, 300.13 MHz; ^{13}C, 75.4 MHz) in C_6D_6 solutions or a Bruker AV 500 (^{31}P, 500.20 MHz) spectrometer in $CDCl_3$ solutions. Chemical shifts were referenced to residue solvent protons at 7.16 ppm (^{1}H NMR) or 128.0 ppm (^{13}C{^{1}H} NMR) for C_6D_6, or to an internal standard at 0 ppm for 85% H_3PO_4 (^{31}P{^{1}H} NMR). Fast atomic bombardment (FAB) mass spectra were measured on a JEOL JMS-700 double focusing mass spectrometer with 3-nitrobenzyl alcohol as matrix. Electrospray (ESI) mass spectra were collected on a Finigan LCQ mass spectrometer (Thermo Finnigan, San Jose, CA, USA) or a Q-Star Pulsari mass spectrometer equipped with a Q-TOF analyzer (Applied Biosystem). MALDI-TOF mass spectra were obtained on a Voyager DE-PRO (Applied Biosystem) equipped with a nitrogen laser (337 nm) and operated in the delayed extraction reflector mode. Fluorescence emission spectra were measured by the ISS PC1™ Photon Counting Spectrofluorometer (ISS, Inc. Champaign, USA). Melting points were recorded on an Electrothermal melting point apparatus and were uncorrected. Elemental analyses were performed by MEDAC Ltd., Brunel University, UK.

UV-vis spectroscopy. Low-temperature optical spectra were measured by a Hewlett-Packard 8453 diode array spectrophotometer equipped with a custom-designed fiber-optic immersion quartz probe of 10 mm path length (Hellma). The immersion probe was fitted to a Schlenk flask (50 cm^3) containing sample solutions. The Schlenk flask was kept inside a Dewar flask, which contained a cold acetone bath. Sample temperature was controlled by a Neslab Cryocool System. The temperature variation was maintained within ±1 °C.

Electrochemistry. Cyclic voltammetry was carried out using a BAS CV-50 W voltammetric analyzer. The electrochemical cell used in our studies consisted of a platinum ball working electrode, a silver wire reference electrode, and a platinum foil auxiliary electrode. All samples solutions were prepared in CH_2Cl_2 with (^{n}Bu$_4$N)(PF_6) (0.15 M) as the supporting electrolyte. Chemical potentials were internally referenced to the $FeCp_2^+/FeCp_2$ redox couple.

X-Ray absorption spectroscopy. X-Ray absorption spectroscopy was performed at the National Synchrotron Radiation Research Center (NSRRC) in Hsinchu (Taiwan) using a Si(111) double crystal monochromator with a beam line Wiggler 17C, 1.5 GeV. Samples were placed inside a sample holder (1.4 cm × 1.4 cm × 0.2 cm) equipped with a septum port and covered with sheets of Kapton. The samples were prepared in separate reaction flasks and were rapidly transferred to the sample holder *via* a cannula. The samples were stored at liquid nitrogen temperature before use. Fluorescence data were measured using an Ar-filled ionization chamber detector equipped with a Ni filter and Soller slits. Data represented an average of 10 scans. Data reduction included energy calibration assigning the first inflection point of the Cu foil to 8980.3 eV, pre-edge subtraction using a polynomial function spline and normalization.

EPR spectroscopy. X-Band EPR spectra were recorded on a Bruker E500 spectrometer equipped with a Bruker TE102 cavity. Sample temperature was maintained at 3.5–40 K using a variable temperature helium flow cryostat system (Oxford Instruments) or at 77 K using a finger Dewar filled with liquid nitrogen. Samples were transferred rapidly from a reaction flask (cooled at 193 K), *via* a cannula, to a degassed EPR tube and frozen immediately with liquid nitrogen.

Quantitation of copper content in the samples was performed by double integration of the first-derivative spectra in the range of 2000–4000 G after base-line corrections. The spin concentrations of the signal due to Cu(II) were determined from a calibration curve using copper(II) nitrate or copper(II) chloride solutions (0.5, 1.0, 1.5 and 2.0 mM in 1 : 1 v/v glycerol/water) as standards.

Determination of hydrogen peroxide

Hydrogen peroxide assay with Ampex Red reagent. To a freshly prepared solution of the bis(μ-iodo)peroxodicopper(II) complex **2** (5–10 μmol) in CH_2Cl_2 at 193 K was added 10 equiv. of HBF_4/Et_2O. An aliquot of 1–5 μL of this acidified solution was added to an aqueous sodium phosphate buffer (pH = 7.4) which contained Ampex Red reagent and horseradish peroxidase to give a final volume of 1.0 mL. The sample solution was incubated at 298 K for 15 min and its fluorescent intensity in the range of 540–700 nm (with excitation at 530 nm) was measured. The concentrations of H_2O_2 in standard solutions were 1–5 μM.

Iodometry. In a typical experiment, a freshly prepared solution of the bis(μ-iodo)peroxodicopper(II) complex **2** (10–20 μmol) in CH_2Cl_2 at 193 K was treated with 10 equiv. of HBF_4/Et_2O. The dark green solution turned bright green. The reaction mixture was stirred at 298 K for 20 min, followed by the addition of diethyl ether to precipitate all copper(II) products. The clear supernatant solution was transferred, *via* a cannula, to a solution of KI in a degassed mixture of acetic acid and distilled water. The resulting yellow mixture was stirred at room temperature for 5 min and then titrated with 0.01 N $Na_2S_2O_3$ until a colorless endpoint was reached.

Synthesis

[Cu(L)(μ-I)]$_2$ (1). Triethylamine (0.14 mL, 1.0 mmol) was added dropwise to a solution of L (0.42 g, 1.0 mL) in dry THF at 0 °C under nitrogen. The resulting yellow solution was stirred for 5 min, and then added dropwise to a slurry of CuI (0.19 g, 1.0 mmol) in dry THF at 0 °C to give a bright yellow mixture. The reaction mixture was stirred overnight at room temperature and then filtered. The yellow filtrate was evaporated *in vacuo* to give the title compound as a yellow solid. Recrystallization of the crude product from dry methanol afforded colorless, block-shaped crystals. Yield: 0.48 g (80%). M.p.: 162–163 °C. ^{1}H NMR (300 MHz, C_6D_6): δ 10.46 (s, 2H, OH), 9.35 (d, J = 3.0 Hz, 4H,

pyridyl), 7.54 (dt, $J = 3.0$ Hz, 2H, Ar), 6.94 (dt, $J = 2.0$, 7.5 Hz, 4H, pyridyl), 6.79 (m, 6H, Ar and pyridyl), 6.59 (t, $J = 6.0$ Hz, 4H, pyridyl), 3.87 (s, 8H CH2), 3.45 (s, 4H, CH_2), 1.75 (s, 18H, But), 1.33 (s, 18H, But). ^{13}C NMR (75.4 MHz, C_6D_6): δ 156.2, 154.8, 151.9, 141.2, 137.0, 136.3, 125.9, 124.8, 123.6, 123.1, 121.7, 58.7, 56.1, 35.4, 34.4, 32.0, 30.1. Anal. Found: C, 52.42; H, 6.28; N, 6.17%. Calcd. for $C_{54}H_{70}I_2N_6O_2Cu_2{\cdot}2CH_3OH$: C, 52.54; H, 6.14; N, 6.56%.

[Cu(L)(μ-I)]$_2$O$_2$ (2). The complex was generated *in situ* by bubbling dry oxygen gas into a stirring solution of [Cu(L)(μ-I)]$_2$ (**1**) in anhydrous CH_2Cl_2 for ~10–20 min at 193 K. The reaction mixture turned immediately from pale yellow to purple, and then deep green. The concentrations of the precursor complex **1** used in this study were 0.1–4 mM.

[Cu(PPh$_3$)$_3$I]·CH$_2$Cl$_2$ (3·CH$_2$Cl$_2$). A solution of **2** was generated *in situ* from [Cu(L)(μ-I)]$_2$ (**1**) (18 mg, 0.015 mmol) and excess dioxygen at 193 K. A stream of argon gas was purged into this solution at 193 K for 15 min to achieve an *anaerobic* condition. A solution of excess PPh_3 (39 mg, 0.15 mmol) in CH_2Cl_2 (1 mL) was added and the reaction mixture was stirred at 193 K for another 10 min. The resulting green solution was allowed to warm to room temperature, whereupon a pale yellow solution was obtained. The solution was EPR silent at 77 K and its electronic spectrum showed no absorption in the 350–900 nm region. Upon standing the solution at room temperature for a few days, pale yellow microcrystals of **3**·CH_2Cl_2 were isolated (5 mg, 35%). The product was washed with Et_2O and dried *in vacuo*. Anal. Found: C, 61.95; H, 4.50%. Calcd. for $C_{54}H_{45}CuIP_3{\cdot}CH_2Cl_2$: C, 62.19; H, 4.46%.

[Cu(L)Cl]Cl·2CHCl$_3$ (4·2CHCl$_3$). A solution of [Cu(PPh$_3$)$_3$I] was obtained by the reaction of **2** with PPh_3 in CH_2Cl_2 as described above. Removal of all the volatiles *in vacuo* led to a crude product, which was characterized by NMR spectroscopy: $^{31}P\{^1H\}$NMR (500 MHz, $CDCl_3$): δ −5.3 (PPh_3), 29.18 (O=PPh_3). The crude product was dissolved in chloroform to give a yellow solution. Standing the solution at room temperature for a few weeks resulted in a color change from yellow gradually to green, and from which green crystals were isolated. The compound was washed with Et_2O and dried *in vacuo*. The empirical formula of the title compound was consistent with results obtained from microanalysis. Anal. Found: C, 44.05; H, 4.72; N, 5.31%. Calcd. for $C_{27}H_{35}Cl_2CuN_3O{\cdot}2CHCl_3$: C, 43.89; H, 4.78; N, 5.66%. The selected bond distances (Å) and angles (°) for the complex are summarized in Table S1.†

Reaction of 2 with PPh$_3$

In a typical experiment, complex **1** (12 mg, 0.01 mmol) was treated with excess dioxygen at 193 K to afford the corresponding bis(μ-iodo)peroxodicopper(II) complex **2** as described above. To achieve *anaerobic* conditions, the solution was purged with a stream of argon for 15 min at 193 K. The solution was allowed to warm to an appropriate temperature (243–288 K) for OAT experiments. A solution of excess PPh_3 (10 equiv. with respect to the precursor complex **1** in CH_2Cl_2 (1 mL) was introduced to the solution by a cannula and the reaction mixture was stirred for 3–18 h, after which time the resulting mixture was quenched with 30% ammonia, followed by a repetitive extraction with CH_2Cl_2. The extract was dried over $MgSO_4$, filtered, and concentrated under reduced pressure. The presence of O=PPh_3 in the product mixture was identified by GC/GC-MS analysis, using *trans*-stilbene oxide as an internal standard with the following temperature profile: injector temperature: 150 °C, initial column temperature: 150 °C (for 1 min), then increasing at a rate of 20 °C min^{-1} to 250 °C (maintained for 16 min). Retention times t_R: PPh_3, 13.2 min (m/z = 262, M^+); O=PPh_3, 21.7 min (m/z = 278, M^+); ^{18}O=PPh_3, 21.7 min (m/z = 280, M^+). The ratio of O=PPh_3 : PPh_3 in a product mixture was also determined by $^{31}P\{^1H\}$ NMR.

Kinetics of the reaction between **2** and PPh_3 in CH_2Cl_2 solutions at 288 K have been studied by following the time dependence of the absorbance at 334 nm due to **2**. Complex **2** was prepared *in situ* by the reaction of the precursor [Cu(L)(μ-I)]$_2$ (**1**) with dry oxygen (as described above) in a reaction vessel equipped with a fiber-optic quartz probe and a stir bar. The concentration of complex **1** was kept at 0.1–0.2 mM. In a typical kinetic measurement, an aliquot (5 mL) of a solution of **1** in CH_2Cl_2 was added to a reaction flask containing 40–50 mL of degassed CH_2Cl_2, followed by bubbling of a precooled oxygen gas through the solution for 10 min at 288 K to accomplish the formation of **2**. Then, an aliquot (0.5 mL) of a solution of PPh_3 in CH_2Cl_2 was introduced, *via* a cannula, into the reaction mixture and the rate of the OAT reaction was monitored. For anaerobic conditions, excess dioxygen in the reaction flask was removed by purging argon gas into the solution for 20 min. During the purging of argon gas, no spectral change of the solution was observed. Analysis of the kinetic data was performed by using the software Origin 6.0 Professional Microcal Software.

X-Ray crystallographic analysis

Single crystals of the solvated complex **1**·2CH_2Cl_2 were obtained from a dichloromethane solution. Crystals suitable for crystallographic studies were mounted in Lindemann glass capillaries and sealed under nitrogen. Data were collected using graphite-monochromatized Mo-K_α radiation ($\lambda = 0.71073$ Å) on a Bruker SMART CCD diffractometer at 293 K using frames of oscillation range 0.3°, with $2.19° < \theta < 28.02°$. Diffraction measurements for a single crystal of **4**·2$CHCl_3$ were carried out with a Bruker-Nonius Apex CCD diffractometer at 100 K using graphite-monochromatized Mo-K_α radiation ($\lambda = 0.71073$ Å) and frame of oscillation range 0.5°, with $2.30° < \theta < 27.48°$. An empirical absorption correction was applied using the SADABS program.[30] The crystal structures were solved by the direct methods and refined by full-matrix least squares on F^2 using the SHELXTL program package.[31]

CCDC reference numbers 285531 and 286337.

For crystallographic data in CIF or other electronic format see DOI: 10.1039/b513898a

Acknowledgements

This work was supported by Academia Sinica and by grants from the National Science Council (NSC 90-2113-M-001-006, 90-2113-M-001-080 and 91-2113-M-006-006). The part of the work done in Hong Kong was supported by a Direct Grant (A/C 2060271) of The Chinese University of Hong Kong. We are grateful to Dr Jyh-Fu Lee of the Research Division of the National Synchrotron Radiation Research Center (NSRRC), Hsinchu, Taiwan for his

kind assistance in the X-ray absorption measurements. Miss H.-W. Li and Professor Thomas C. W. Mak of CUHK solved the X-ray structure of $[CuL(\mu\text{-}I)]_2 \cdot 2CH_2Cl_2$, and Mr Yuh-Sheng Wen solved the X-ray structure of $[Cu(L)Cl]Cl \cdot 2CHCl_3$. We are indebted to these colleagues for their contributions to the work. Finally, one of us (H.K.L.) would like to thank Dr Yee-Lok Wong for helpful discussions on the synthesis of **1**; and S.V.P. and S.I.C. are grateful to Dr Peter P.-Y. Chen for discussions on the interpretation of the EPR results.

References

1 G. Davies and M. A. El-Sayed, in *Copper Coordination Chemistry: Biochemical and Inorganic Perspectives*, ed. K. D. Karlin and J. Zubieta, Adenine, Guilderland, NY, 1983, p. 281 and ref. therein.
2 K. G. Caulton, G. Davies and E. M. Holt, *Polyhedron*, 1990, **9**, 2319–2351 and ref. therein.
3 M. A. El-Sayed, A. El-Toukhy and G. Davies, *Inorg. Chem.*, 1985, **24**, 3387–3390.
4 G. Davies, M. A. El-Sayed and M. Henary, *Inorg. Chem.*, 1987, **26**, 3266–3273 and ref. therein.
5 M. A. El-Sayed, G. Davies and T. S. Kasem, *Inorg. Chem.*, 1990, **29**, 4730–4735.
6 M. A. El-Sayed, K. Z. Ismail, T. A. El-Zayat and G. Davies, *Inorg. Chim. Acta*, 1994, **217**, 109–119.
7 S. M. Carrier, C. E. Ruggiero, R. P. Houser and W. B. Tolman, *Inorg. Chem.*, 1993, **32**, 4889–4899.
8 M. Mizuno, H. Hayashi, S. Fujinami, H. Furutachi, S. Nagatomo, S. Otake, K. Uozumi, M. Suzuki and T. Kitagawa, *Inorg. Chem.*, 2003, **42**, 8534–8544.
9 H. Hayashi, K. Uozumi, S. Fujinami, S. Nagatomo, K. Shiren, H. Furutachi, M. Suzuki, A. Uehara and T. Kitagawa, *Chem. Lett.*, 2002, 416–417.
10 L. M. Mirica, X. Ottenwaelder and T. D. P. Stack, *Chem. Rev.*, 2004, **104**, 1013–1045 and ref. therein.
11 W. Shin, U. M. Sundaram, J. L. Cole, H. H. Zhang, B. Hedman, K. O. Hodgson and E. I. Solomon, *J. Am. Chem. Soc.*, 1996, **118**, 3202–3215.
12 K. D. Karlin, R. W. Cruse and Y. Cultneh, *J. Chem. Soc., Chem. Commun.*, 1987, 599–600.
13 S. Teramae, T. Osako, S. Nagatomo, T. Kitagawa, S. Fukuzumi and S. Itoh, *J. Inorg. Biochem.*, 2004, **98**, 746–757.
14 E. I. Solomon, B. L. Hemming and D. E. Root, in *Bioinorganic Chemistry of Copper*, Chapman & Hall, New York, 1993, pp. 3–21.
15 E. I. Solomon, F. Tuczek, D. E. Root and C. A. Brown, *Chem. Rev.*, 1994, **94**, 827–856.
16 P. P. Paul, Z. Tyeklár, R. R. Jacobson and K. D. Karlin, *J. Am. Chem. Soc.*, 1991, **113**, 5322–5332.
17 M. R. Churchill, G. Davies, M. A. El-Sayed, J. A. Fournier, J. P. Hutchinson and J. A. Zubieta, *Inorg. Chem.*, 1984, **23**, 783–787.
18 J. Li, S. Yao, H. Chen and Y. Zhang, *Spectrosc. Lett.*, 1996, **29**, 1563–1572.
19 P. Weinberger, O. Costisor, R. Tudose, O. Baumgartner and W. Linert, *J. Mol. Struct.*, 2000, **519**, 21–31.
20 G. Herzberg, *Spectra of Diatomic Molecules*, D. Van Nostrand Co., New York, 1950, 2nd edn, p. 171.
21 L.-S. Kau, D. J. Spira-Solomon, J. E. Penner-Hahn, K. O. Hodgson and E. I. Solomon, *J. Am. Chem. Soc.*, 1987, **109**, 6433–6442.
22 B. Lucchese, K. J. Humphreys, D.-H. Lee, C. D. Incarvito, R. D. Sommer, A. L. Rheingold and K. D. Karlin, *Inorg. Chem.*, 2004, **43**, 5987–5998.
23 S. V. Pavlova, K. H.-C. Chen and S. I. Chan, *Dalton Trans.*, 2004, 3261–3272.
24 S. I. Chan, K. H.-C. Chen, S. S.-F. Yu, C.-Li Chen and S. S.-J. Kuo, *Biochemistry*, 2004, **43**, 4421–4430.
25 Y. Shimazaki, S. Huth, S. Hirota and O. Yamauchi, *Bull. Chem. Soc. Jpn.*, 2000, **73**, 1187–1195.
26 Y.-L. Wong, *PhD Thesis*, The Chinese University of Hong Kong, 1999.
27 D. D. Perrin and W. L. F. Armarego, *Purification of Laboratory Chemicals*, Pergamon Press, New York, 1988.
28 R. Battino, *Oxygen and Ozone*, ed. R. Battino, Pergamon Press, New York, 1981, vol. 7.
29 S. V. Kryatov, E. V. Rybak-Akimova, V. L. MacMurdo and L. Que, Jr., *Inorg. Chem.*, 2001, **40**, 2220–2228.
30 G. M. Sheldrick, *SADABS: Program for Empirical Absorption Correction of Area Detector Data*, University of Göttingen, Germany, 1996.
31 G. M. Sheldrick, *SHELXTL 5.10 for Windows NT: Structure Determination Software Programs*, Bruker Analytical X-Ray Systems, Inc., Madison, Wisconsin, USA, 1997.